J Mater Sci: Mater Med (2008) 19:2799–2807
DOI 10.1007/s10856-007-3356-3

Synthesis of gelatin-containing PHBV nanofiber mats for biomedical application

Wan Meng · Zhi-Cai Xing · Kyung-Hye Jung · Se-Yong Kim · Jiang Yuan · Inn-Kyu Kang · Sung Chul Yoon · Hong In Shin

Received: 9 July 2007 / Accepted: 28 December 2007 / Published online: 6 March 2008

Abstract Electrospinning is one of the fabrication method to form ultra-fine fiber in a nano-scale made of synthetic and natural extracellular matrix components for tissue-engineering applications. In this study, a nanofibrous scaffold was obtained by co-electrospinning poly (3-hydroxybutyrate-co-3-hydroxyvalerate) (PHBV) and gelatin in 2,2,2-trifluoroethanol (TFE) at a ratio of 50/50. The resulting fiber diameters were in the range of 400–1,000 nm without any beads. The nanofiber surfaces were characterized by attenuated total reflection-Fourier transform infrared spectroscopy (ATR-FTIR), electron spectroscopy for chemical analysis (ESCA), and atomic force microscopy. It was found, from cell culture experiments, that NIH 3T3 cells on the PHBV/gelatin nanofibrous scaffold more proliferated than on the PHBV nanofibrous scaffold.

Keywords Gelatin · PHBV · Nanofibers · Tissue engineering

W. Meng · Z.-C. Xing · K.-H. Jung · S.-Y. Kim · J. Yuan · I.-K. Kang (✉)
Department of Polymer Science, Kyungpook National University, Daegu 702-701, Republic of Korea
e-mail: ikkang@bh.knu.ac.kr

W. Meng
Department of Chemical Engineering and Polymer Science, Yanbian University, Yanji 133002, People's Republic of China

S. C. Yoon
Department of Microbiology, Gyeongsang National University, Chinju 660-701, Republic of Korea

H. I. Shin
School of Dentistry, Kyungpook National University, Daegu, Republic of Korea

1 Introduction

Restoration of organ function utilizing tissue engineering requires the use of a three-dimensional scaffold. The scaffold should be mechanically stable and capable of functioning biologically in the implant site [1]. Recently, a variety of techniques have been developed for nano- or submicron fiber fabrication, including phase separation [2, 3], electrospinning [4], and self-assembly [5]. Among them, electrospinning provides a straightforward way to fabricate fibrous scaffolds with nano-sized diameter fibers, which mimic the structure of natural extracellular matrix (ECM) [6].

To date, electrospinning has been used for the fabrication of ultra-thin fibrous scaffolds from biodegradable synthetic polymers, such as poly (lactic acid) (PLA) [7, 8], poly(glycolic acid) (PGA) [9], poly (lactide-*co*-glycolide) (PLGA) [4, 10], and poly (ε-caprolactone) (PCL) [11]. Very recently, some natural biopolymers, which include silk [12, 13], fibrinogen [14], collagen [15], and gelatin [16, 17] have also been successfully electrospun. Compared to synthetic polymers, natural biopolymers have good biocompatibility. However, in general, their processability is rather poor [18].

Poly (3-hydroxybutytric acid-*co*-3-hydroxyvaleric acid) (PHBV) is a well known biodegradable, biocompatible, non-toxic and thermoplastic polyester produced by bacteria [19]. PHBV is being developed and commercialized as an ideal substitute for non-biodegradable polymeric materials in commodity applications because of its biodegradability and easy processability.

Among the natural biopolymers, gelatin can be obtained by denaturing collagen and has almost identical composition and biological properties as those of the parent collagen. Much attention has been focused on the use of gelatin as a tissue engineering material due to its low cost.

In this study, gelatin and PHBV were co-electrospun to produce PHBV/gelatin composite fibrous scaffold. The characteristics of nanofibrous scaffold were examined using ATR-FTIR spectroscopy, electron spectroscopy for chemical analysis (ESCA), and atomic force microscopy (AFM). The biological performance of the nanofibrous scaffolds was also studied.

2 Materials and methods

2.1 Materials

Poly (3-hydroxybutyric acid-*co*-3-hydroxyvaleric acid) (PHV content: 5 wt%; PHBV) and gelatin type B were purchased from Aldrich Chemical Co., USA. 2,2,2-Trifluoroethanol (TFE) was purchased from TCI, Japan.

2.2 Film casting

Solvent casting PHBV film served as the control substrate in the cell adhesion studies. To prepare the film, 10 ml PHBV/TFE solution was spread on a glass plate and the solvent was evaporated at room temperature. The concentrated PHBV solution was then irradiated by an infrared lamp to evaporate the residual solvent.

2.3 Preparation of polymer Solution

A transparent polymer solution was prepared by dissolving gelatin and PHBV in TFE with sufficient stirring at room temperature. To examine the effect of gelatin content on fiber morphology, a 6 wt% polymer solution was prepared using different ratios of PHBV and gelatin. In order to examine the affect of polymer concentration on fiber morphology, a PHBV/gelatin (50/50) blend was dissolved using TFE to prepare several solutions with concentrations ranging from 2 to 8 wt%.

2.4 Electrospinning

Electrospinning was carried out according to the procedure detailed by Li et al. [4]. Briefly, the polymer solution was delivered to a metal needle connected to a high voltage power supply (Chungpa EMT, Seoul, Korea). Upon applying a high voltage, a fluid jet was ejected from the needle. As the jet accelerated towards a grounded collector, the solvent evaporated and a charged polymer fiber was deposited on the collector in the form of a nanofibrous scaffold. The polymer solutions were electrospun with 2.0 ml/h of a mass flow rate, 7 kV of voltage, and 12 cm of the distance between the tip and the collector. After electrospinning, all nanofibrous scaffolds were placed in a vacuum drying oven at room temperature for several days of drying treatment.

2.5 Surface characterization

The ATR-FTIR spectra of the nanofibrous scaffolds were obtained using an FT-IR Spectrometer (Jasco-620, Tokyo, Japan). The electrospun scaffolds were analyzed using ESCA (ESCA LAB VG microtech, Mt 500/1 etc, East Grin, UK) equipped with Mg Kα at 1,253.6 eV and 150 W power at the anode. A survey scan spectrum was taken and the surface elemental compositions relative to carbon were calculated from the peak height with a correction for atomic sensitivity.

For analysis of the morphology of the electrospun fibers, the samples were sputter-coated with gold and examined using a field-emission scanning electron microscope (FE-SEM, Hitachi S-4300, Japan). The diameter of the electrospun nanofibers was measured using an image analyzer (TDISE V3.1.73).

Surface properties of the nanofibers were examined using a Nanoscope IIIa atomic-force microscope (Digital Instruments, Santa Barbara, CA), in phase mode, in air, and using a square pyramidal tip of a Si3N4 cantilever.

2.6 In vitro biodegradation of nanofibrous scaffolds

For the use in the biodegradation study, the solutions were electrospun for 5 h at a flow rate of 2.0 ml/h to obtain PHBV and PHBV/gelatin nanofiber scaffold with size of 100 × 300 × 0.05 mm. The nanofibrous scaffold was cut into rectangles (20 × 20 × 0.05 mm) for an in vitro biodegradation test. Each specimen was placed in a test tube containing 10 ml of phosphate-buffered saline (PBS, pH 7.0, Gibco, Japan) and incubated for a requisite time at 37°C. After incubation, the samples were washed and lyophilized for 24 h.

To measure the enzymatic degradation of nanofibrous scaffolds, the samples were placed in a PBS containing collagenase type I (10 mg/ml, Wako, Japan) or *Pseudomonas stutzeri* BM190 depolymerase (0.1 mg/ml). After a requisite incubation time, the samples were taken out from the enzyme solution, washed with distilled water and lyophilized for 24 h. Morphological changes of the nanofibrous scaffolds were examined using a field emission scanning electron microscope (FE-SEM; S-4300, Japan).

2.7 Cell culture

To examine the interaction of nanofibrous scaffolds with cells, the circular nanofibrous scaffolds were fitted in a 24-well culture dish and subsequently immersed in a DMEM medium containing 10% fetal bovine serum (FBS) (Gibco, Japan) and 1% penicillin G-streptomycin (Gibco, Japan). One milliliter of NIH 3T3 cell solution (5×104 cells/cm^2) was added to the sample sheet and incubated in a humidified atmosphere of 5% CO_2 at 37°C for 4 h to see the early cell adhesion activity on the nanofibers. After incubation, the supernatant was removed, washed twice with a PBS, and fixed in a 2.5% glutardialdehyde aqueous solution for 20 min. The sample sheet was then dehydrated, dried in a critical point drier, and finally sputter-coated with gold. The surface morphology of the samples was then observed with an FE-SEM.

2.8 BrdU assay for cell proliferation

The proliferation of NIH 3T3 cells seeded on the nanofibrous scaffolds was determined using a colorimetric immunoassay based on the measurement of 5-bromo-2′-deoxyuridine (BrdU), that were incorporated during DNA synthesis [20, 21]. BrdU ELISA (Roche Molecular Biochemicals, USA) was performed according to the manufacturer's instructions. Briefly, after cell culture for 48 h, BrdU-labeling solution was added to each well and was allowed to incorporate into the cells in a CO_2-incubator at 37°C for a further 20 h. Subsequently, the supernatant in each well was removed by pipetting and washed twice with PBS. The cells were treated with 0.25% trypsin-EDTA (Gibco, Japan) and harvested by centrifugation of the cell solution at 1,000 rpm for 15 min. The harvested cells were mixed with a FixDenat solution to fix the cells and denature the DNA and incubated for 30 min. Subsequently, the diluted anti-BrdU-peroxidase (dilution ratio = 1:100) was added and kept at 20°C for 120 min. After removing the unbound antibody conjugate, 100 µl of substrate solution were added, allowed to stand for 20 min, and the reaction was completed by adding 25 µl H_2SO_4 solution (1 M). The solution was transferred to a 96-well plate and measured within 5 min at 450 nm with a reference wavelength of 690 nm, using an ELISA plate reader (EL × 800). The blank corresponded to 100 µl of culture medium with or without BrdU.

2.9 Cell viability

A 3-(4,5-dimethylthiazol-2-yl)-2,5-diphenyl-tetrazolium bromide (MTT) (Sigma, USA) assay was used to measure relative cell viability [22, 23]. After 7 days incubation on the nanofibrous scaffolds, cell viability was evaluated using an MTT assay. Shortly, 50 µl of a MTT solution (5 mg/ml in PBS) was added to each well and incubated in a humidified atmosphere of 5% CO_2 at 37°C for 4 h. After removing the medium, the converted dye was dissolved in acidic isopropanol (0.04 N HCl–isopropanol) and kept for 30 min in the dark at room temperature. Hundred microliter of the medium was taken from each sample, transferred to a 96-well plate, and subjected to ultraviolet measurements of converted dye, at a wavelength of 570 nm, on a kinetic microplate reader (EL × 800, Bio-Tek® Instruments, Inc, Highland Park, USA). It was revealed, in preliminary experiments, that gelatin nanofibers were partially dissolved in an aqueous solution, and easily lost their fibrous structure. However PHBV/gelatin (5:5) composite nanofibers were stable in an aqueous medium.

2.10 Statistical analysis

Results are displayed as mean ± standard deviation. Statistical differences were determined by a student's two-tailed t test. Scheffe's method was used for multiple comparison tests at a level of 95%.

3 Results

3.1 Electrospinning

To evaluate the effect of the dope composition and concentration, electrospinning was performed with various composite ratios (PHBV/gelatin at ratio of 30/70, 50/50, 70/30) and different polymer concentrations (2, 4, 6, 8 wt%). The morphological structures of electrospun PHBV/gelatin nanofibers in different mixing ratio are shown in Fig. 1. As shown in the SEM photographs of Fig. 1, a very uniform and finest nanofiber could be obtained at different mixing ratios. To consider the mechanical properties and biocompatibility of nanofibrous scaffold, 50/50 mixing ratio of dope solution was fixed.

Figure 2 shows PHBV/gelatin nanofiber depending on the concentration of 2–8 wt% at 50/50 mixing ratio. At a concentration of 4 and 6 wt%, continuous nanofibers without beads could be obtained. As the content of gelatin and the concentration of solutions increased, the diameter of nanofibers was getting thicker and the distribution of fibers was getting broader. In this study, a 6 wt% (50/50) concentration of polymer solution was fixed throughout further experiments.

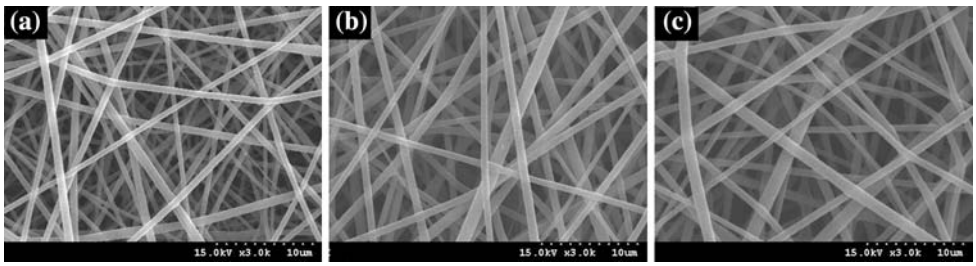

Fig. 1 SEM micrographs of electrospun fibers using PHBV/gelatin solution in TFE 6 wt%. (**a**) 30/70, (**b**) 50/50, (**c**) 70/30

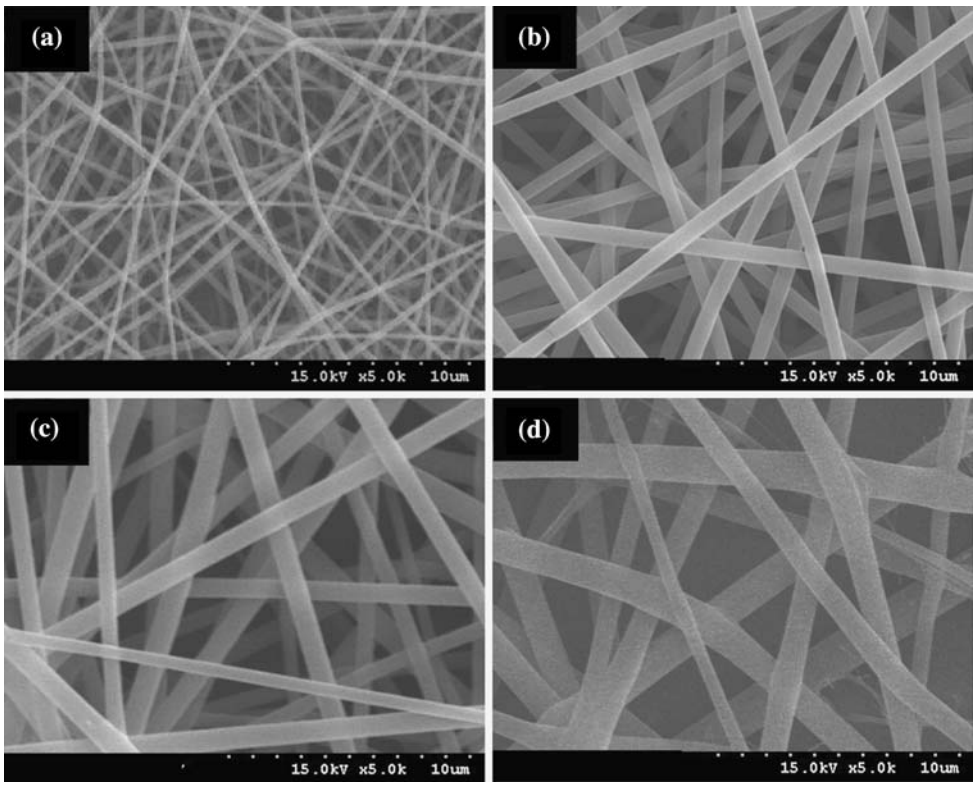

Fig. 2 SEM micrographs of electrospun fibers of PHBV/gelatin (50/50) mat using TFE solutions as a function of concentration. (**a**) 2 wt%, (**b**) 4 wt%, (**c**) 6 wt%, (**d**) 8 wt%

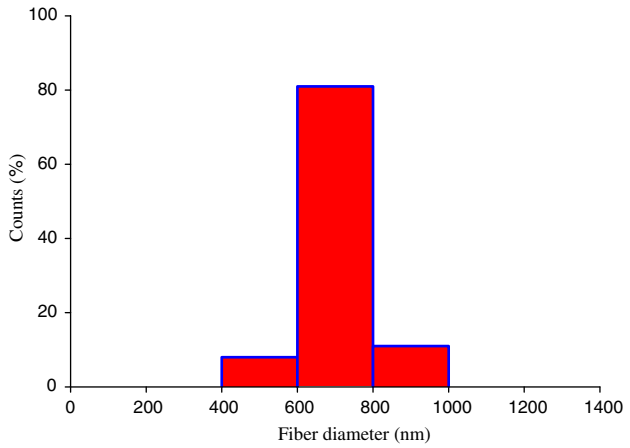

Fig. 3 Diameter distribution of PHBV nanofiber electrospun from 6 wt% PHBV-TFE solution

Image analysis of PHBV/gelatin nanofibers (6 wt%, 50/50) revealed that their diameters ranged from 400 nm to 1 μm, as shown in Fig. 3.

3.2 Characterization of nanofibrous scaffolds

Figure 4 shows the ATR-FTIR spectra of nanofibrous scaffolds. The ATRFTIR spectrum of gelatin (a) showed two characteristic peaks at around 1,650 and 1,540 cm^{-1} based on amide I and II as expected. The spectrum of PHBV/gelatin (Fig. 4b) also showed absorption peaks at around 1,650 and 1,540 cm^{-1}, based on amide I and II of gelatin, corresponding stretching vibration of C=O bond, and coupling of bending of N–H bond and stretching of C–N bond, respectively. The absorption at 1,733 cm^{-1} is attributed to the ester groups of PHBV (Fig. 4c).

Changes in the chemical structure of nanofibrous scaffolds were investigated using ESCA. Figure 5 shows ESCA survey scans of the nanofibrous scaffold surfaces. As expected, the co-electrospun scaffold PHBV/gelatin shows three peaks corresponding to C1s (binding energy, 285 eV), N1s (binding energy, 400 eV), and O1s (binding energy, 532 eV). The chemical compositions of the

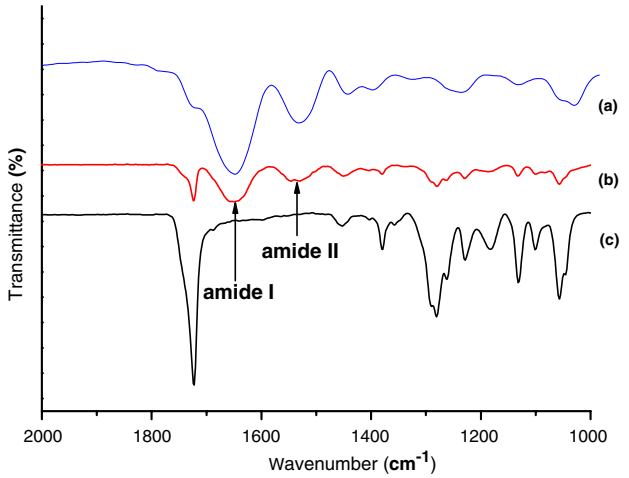

Fig. 4 ATR-FT IR spectra of a gelatin (a), PHBV/gelatin (b) and PHBV (c) nanofiber mats

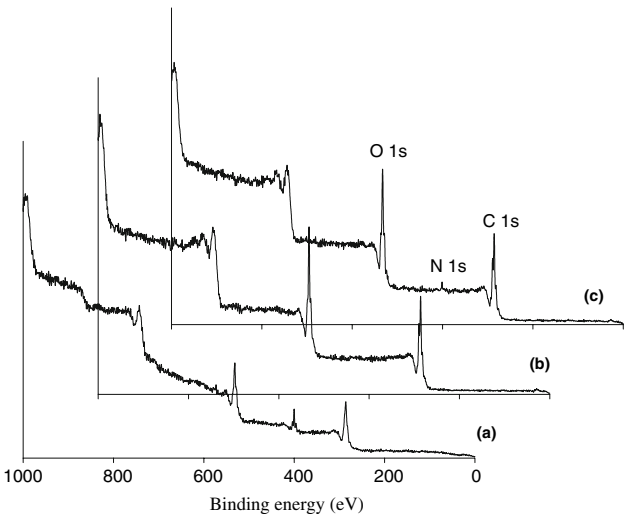

Fig. 5 ESCA survey scan spectra of (a) gelatin nanofiber, (b) PHBV nanofiber, (c) PHBV/gelatin nanofiber

nanofibrous scaffolds calculated from the ESCA survey scan spectra are shown in Table 1. The oxygen content (32%) of the PHBV nanofiber surface was decreased by the incorporation of gelatin (PHBV/gelatin, 25%). On the other hand, nitrogen (7%) was found on the PHBV/gelatin scaffold surface.

To study the surface morphologies of PHBV and PHBV/gelatin nanofiber surfaces, AFM image was examined using a tapping mode and expressed as phase images. On the PHBV nanofiber surface, a relative homogeneous pattern was observed as shown in Fig. 6a. On the PHBV/gelatin nanofiber surface (Fig. 6b) a phase-separated structure appeared showing the distribution gelatin on the PHBV matrix well. The phase-separated structures are probably attributed to the globular structure and hydrophilicity of gelatin.

Table 1 Chemical composition of a nanofiber gelatin, PHBV and PHBV/gelatin (5:5 wt%) mats calculated ESCA

Substrate	Atomic percent (%)		
	C	O	N
Gelatin	44	46	10
PHBV	68	32	0
PHBV/gel	68	25	7

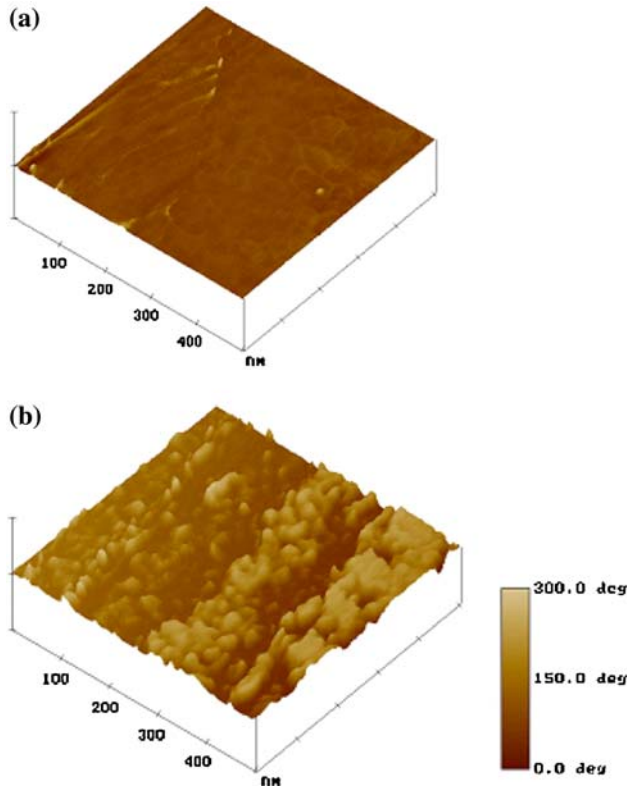

Fig. 6 AFM images represented by phase mode: (**a**) PHBV fiber (**b**) PHBV/gelatin fiber

3.3 In vitro degradation of nanofibrous scaffolds

Figure 7 illustrates the morphological changes on nanofibrous scaffold surfaces after incubation in PBS with or without depolymerase (*Pseudomonas stutzeri* BM190). Before the depolymerase treatment, PHBV/gelatin (Fig. 7a) exhibited a preserved nanofibrous structure. After 4–6 h incubation in depolymerase solution, the PHBV nanofiber showed very high morphological changes (Fig. 7c, d). After collagenase treatment, as shown in Fig. 8, the PHBV/gelatin fibers broke down and partially adhered to each other after 24 and 48 h incubation time.

3.4 Cell-scaffold interaction

As shown in Fig. 9, NIH 3T3 fibroblasts highly spreaded on to the PHBV (Fig. 9c) and PHBV/gelatin scaffold

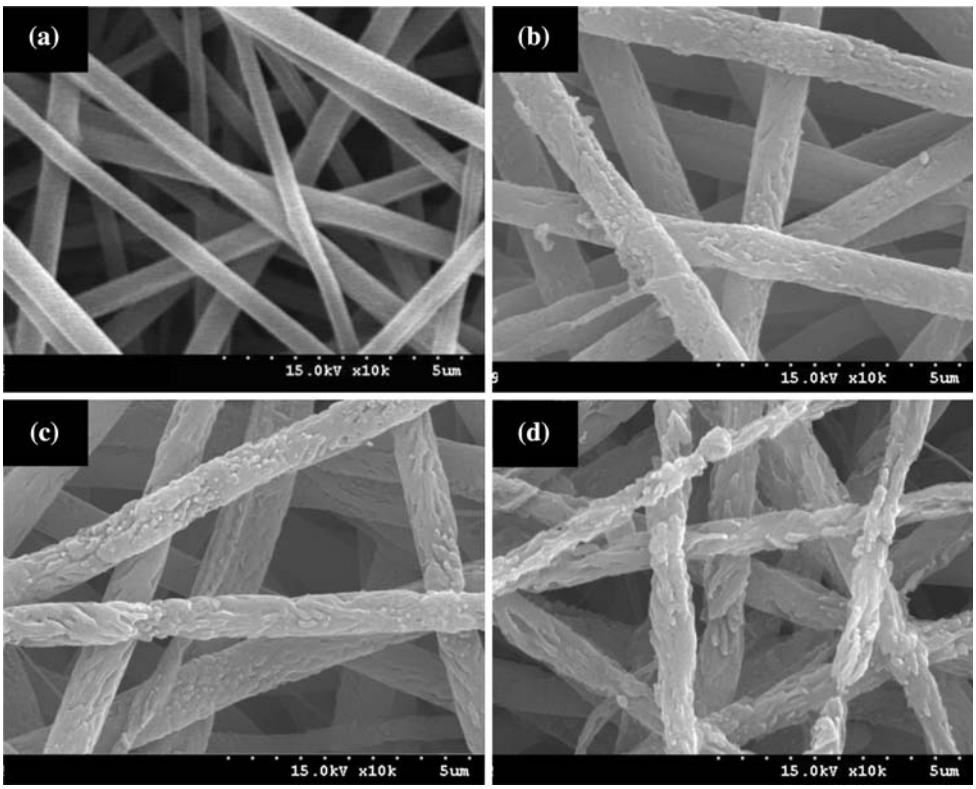

Fig. 7 Biodegradation of PHBV/gelatin (50/50) nanofibrous scaffold by PHB depolymerase solution as a function of incubation time. (**a**) 0 h, (**b**) 1 h, (**c**) 4 h, (**d**) 6 h

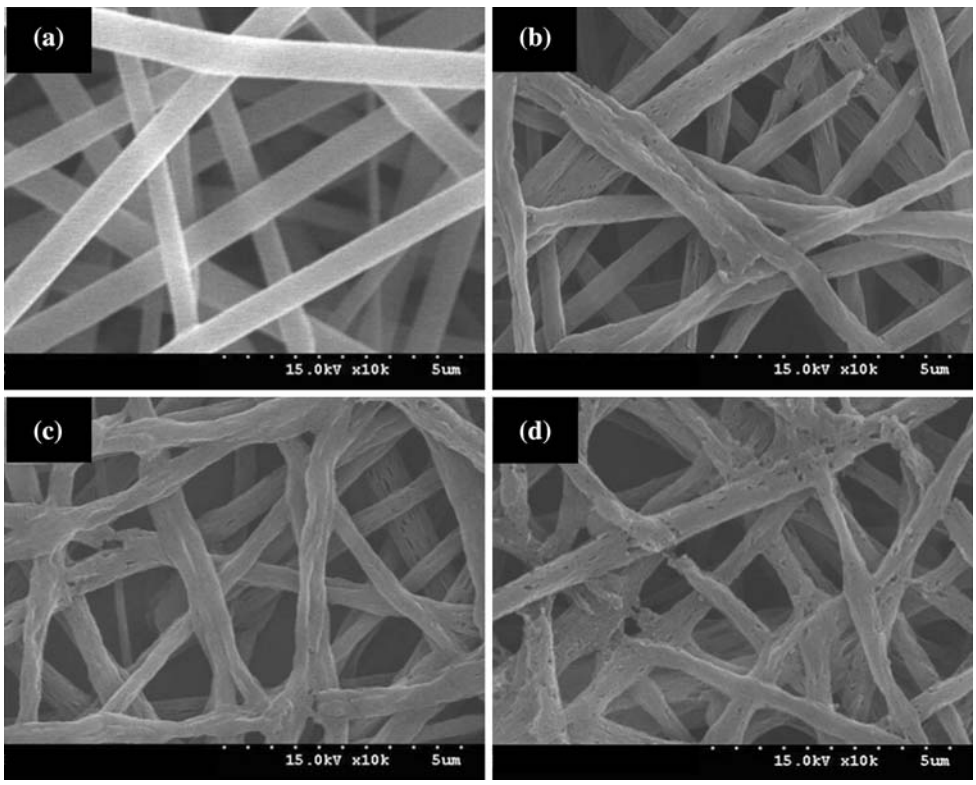

Fig. 8 Biodegradation of PHBV/gelatin nanofibrous scaffold by collagenase solution as a function of incubation time. (**a**) 0 h, (**b**) 12 h, (**c**) 24 h, (**d**) 48 h

(Fig. 9d) compared with culture dish (Fig. 9a) and PHBV film (Fig. 9b) after 4 h incubation. NIH 3T3 fibroblasts cultured on PHBV and PHBV/gelatin nanofibers for 1 day are shown in Fig. 10. As the results, cells adhered to the PHBV/gelatin scaffold (Fig. 10b) more quickly formed monolayer than those to the PHBV nanofibrous scaffold

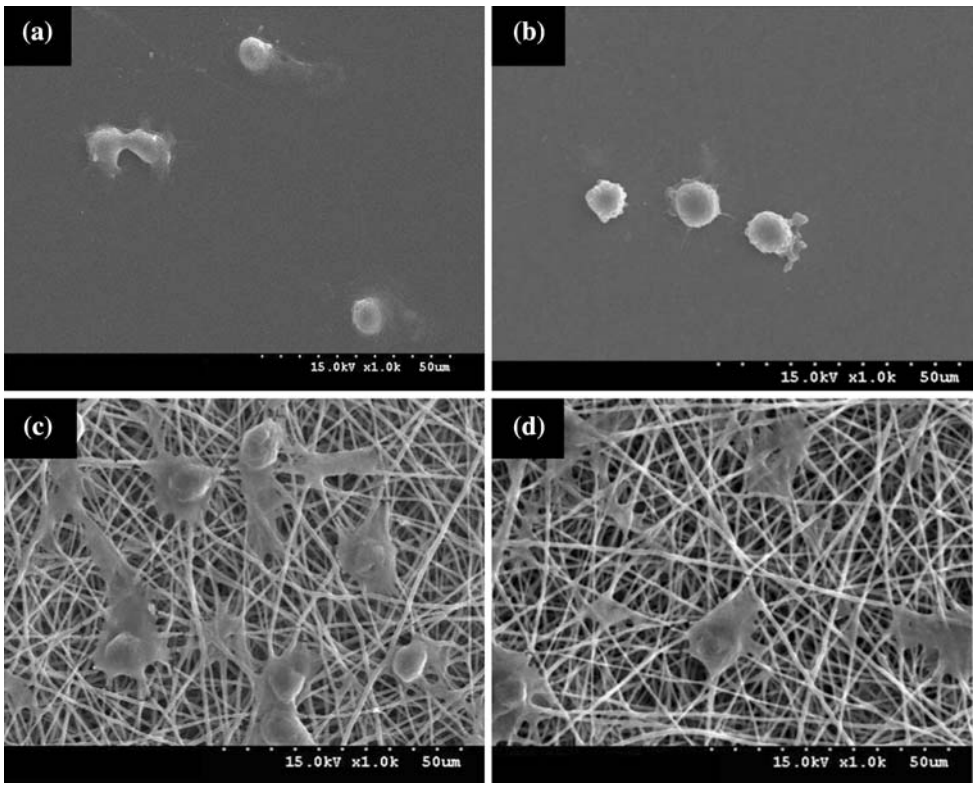

Fig. 9 Adhesion of fibroblasts on culture dish (**a**), PHBV film (**b**), PHBV (**c**) and PHBV/gelatin Nanofibrous scaffold (**d**) for 4 h incubation

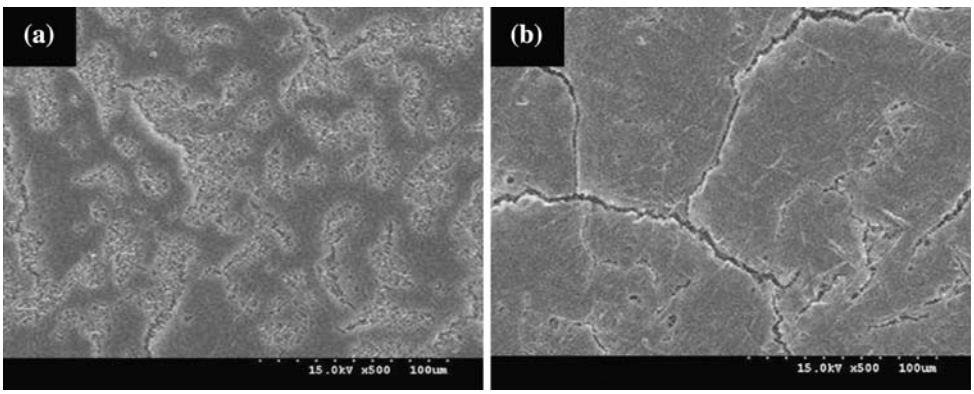

Fig. 10 Morphology of fibroblasts on PHBV (**a**) and PHBV/gelatin Nanofibrous scaffold (**b**) for 1-day incubation

(Fig. 10a), showing a good tissue compatibility of the PHBV/gelatin nanofibrous scaffold.

Figure 11 shows cross section images of PHBV/gelatin scaffold after fibroblasts culture. After 3 days incubation, a monolayer morphology was found. After 6 days incubation, a thicker layer was formed, indicating that the composite scaffold allowed cellular penetration or infiltration into the inside of PHBV/gelatin composite fibrous structure.

Comparable results for differences in proliferation behavior, expressed as the amount of newly synthesized DNA, are shown in Fig. 12. The DNA synthesis of NIH 3T3 cells cultured on the matrices for 24 h revealed that cells could proliferate on all matrices. Compared to PHBV film, fibroblasts proliferation on PHBV nanofibrous scaffold was significantly higher ($p < 0.01$). In addition, the cell proliferation on PHBV/gelatin nanofibrous scaffold was higher than on the PHBV nanofibrous scaffold ($p < 0.05$). An MTT assay was used to measure relative cell viability.

Figure 13 shows the cell viability of fibroblasts seeded on nanofibrous scaffolds for different incubation times. Metabolically active mitochondrial dehydrogenases convert the tetrazolium salt MTT to insoluble purple formazon crystals of which the amount is proportional to cell viability [24]. The value of cell viability (Fig. 13) means the maximum absorption of MTT formazan (570 nm) collected from the cells seeded on nanofiber scaffold. After 3–14 days incubation, the cell viabilities on both PHBV and PHBV/gelatin nanofibrous scaffolds exhibited a similar

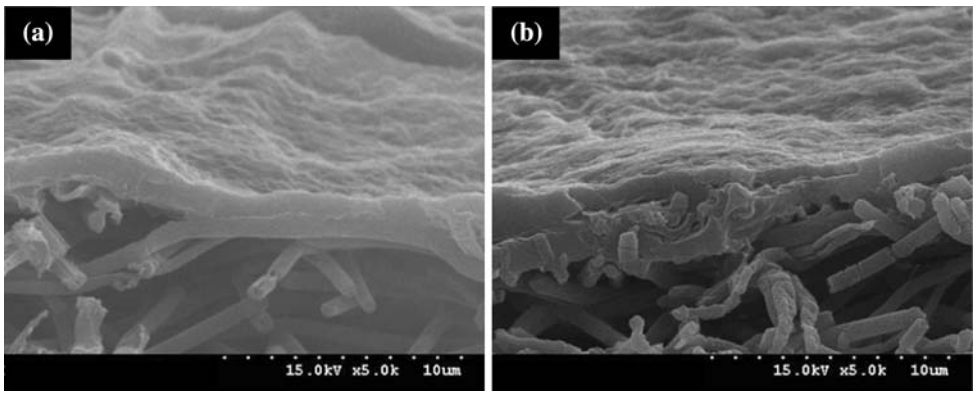

Fig. 11 Cross section image of PHBV/gelatin nanofibrous scaffold after fibroblasts cultured after 3 days (**a**) and 6 days (**b**) incubation

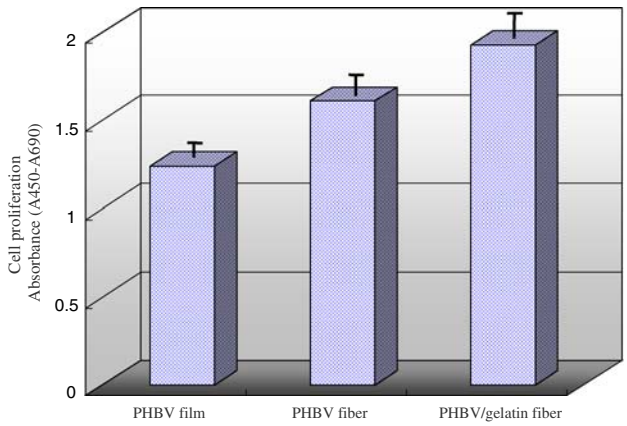

Fig. 12 Assessment of NIH 3T3 cell proliferation using the BrdU ELISA. Data are expressed as mean ± SD ($n = 5$) of the specific absorbance

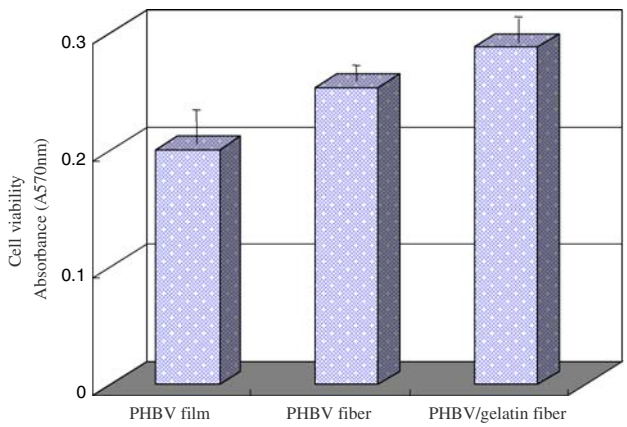

Fig. 13 MTT assay, Formosan absorbance expressed as a measure of cell viability from NIH 3T3 cells cultured onto nanofibrous scaffolds for 5 days. Data are expressed as mean ± SD ($n = 5$) of the specific absorbance

tendency. After 7 days incubation, compared to PHBV film, the cell viability of fibroblasts cultured on PHBV and PHBV/gelatin nanofibrous scaffolds was significantly enhanced ($p < 0.01$).

4 Discussion

The electrospinning technique is widely recognized as a straightforward way to fabricate nanoscale fibrous structures. Since this technique can produce nano- or submicron fibrous scaffolds which mimic the structure of natural ECM, it has elicited extensive research interest [6]. In this study, various polymer concentrations and mixing ratios were used to produce PHBV/gelatin fibrous scaffolds. With increasing concentrations, the fiber diameter of electrospun nanofiber increased, indicating that the diameter increased with the viscosity of the polymer solution due to the proportionality between the concentration and viscosity [25–27]. At a concentration of 6 wt% and a mixing ratio of 50/50, uniform fibers ranging from 400 nm to 1 μm were formed successfully. Huang et al. [28] used co-electrospinning to produce poly (ε-caprolactone) (PCL)/gelatin nanofibrous scaffold and obtained nanofibers ranging from tens of nanometers to approximately 1 μm.

In order to illustrate the presence of gelatin in the co-electrospun scaffolds, a PHBV/gelatin scaffold was subjected to ATR-FTIR measurements. The resulting spectrum yielded peaks that were characteristic of gelatin, as reported previously by other researchers [29].

The enzymatic degradation of PHBV film by PHB depolymerase has been reported previously [30]. Park et al. [31] have carried out biodegradation tests of PHBV in the form of fibrous structures or film, using a simulated municipal solid waste aerobic composting method. They reported that the degradation of PHBV non-woven structures was faster than PHBV film. In the current study, the surface of the PHBV/gelatin fibers was severely eroded by the PHB depolymerase treatment, indicating that the gelatin composite improved wettability of PHBV/gelatin nanofiber surface and increased the enzyme contact with the fiber surface. On the other hand, the PHBV/gelatin fibers were partially biodegraded by treatment with collagenase solution and their cylindrical morphology was severely damaged.

Recently, a great deal of research has focused on the influence of scaffold microarchitecture on cell behavior [11, 32]. Biomedical applications of gelatin [33–35] and collagen [36–38] nanofiber scaffolds have been reported. Shin et al. [39] assessed the interaction of chondrocyte with co-electrospun chitosan/gelatin nanofibrous scaffolds and reported that a porous nanofiber scaffold can maintain chondrocyte proliferation and differentiation and promote cartilage formation. Venugopal et al. reported that PCL-blended collagen nanofibrous membrane has the potential to be applied in tissue engineering [40]. Ito et al. prepared the PHBV nanofibers composited with hydroxyapatite and reported that nanofibrous film showed higher cell adhesion activity than the cast flat film [41]. In the current study, the PHBV/gelatin nanofibrous scaffold accelerated the adhesion and growth of NIH 3T3 cells as compared to the PHBV nanofibrous scaffold.

5 Conclusion

In this study, a three-dimensional structure of PHBV/gelatin composite nanofibrous scaffold was produced by electrospinning. Cell-culture experiments showed that NIH 3T3 cells had very favorable interactions with the PHBV/gelatin composite scaffold compared with PHBV film and a PHBV nanofibrous scaffold. Significantly, cellular infiltration into the PHBV/gelatin composite fibrous scaffold was demonstrated. It is concluded that coelectrospinning ECM with synthetic polymers has many potential applications in tissue-engineering.

Acknowledgements This work was supported by the Ministry of Commerce, Industry and Energy (Grant No. 10015388) and Kyungpook National University Research Team Fund (2003).

References

1. R.C. Thomson, M.J. Yaszemski, A.G. Mikes (Austin, R.G. Landes, 1997)
2. P.X. Ma, R. Zhang, J. Biomed. Mater. Res. **46**, 60 (1999)
3. F. Yang, R. Murugan, S. Ramakrishina, X. Wang, Y.W. Ma, S. Wang, Biomaterials **25**, 1891 (2003)
4. W.J. Li, C. Laurencin, E. Caterson, R. Tuan, F. Ko, J. Biomed. Mater. Res. **60**, 613 (2003)
5. J.D. Hartgerink, E. Beniash, S.I. Stupp, Science **294**, 1684 (2001)
6. F. Yang, C.Y. Xu, M. Kotaki, S. Wang, S. Ramakrishna, J. Biomater. Sci. Polmer. Edn. **15**, 1483 (2004)
7. K.S. Kim, M. Yu, X. Zong, J. Chiu, D. Fang, Y.S. Seo, B.S. Hsiao, B. Chu, M. Hadjiargyrou, Biomaterials **24**, 4977 (2003)
8. J. Zeng, X. Chen, X. Xu, Q. Liang, X. Bian, L. Yang, X. Jing, J. Appl. Polym. Sci. **89**, 1085 (2003)
9. E. Boland, G. Wnek, D. Simpson, K. Pawlowski, G.J. Bonlin, Macromol. Sci. Part A Pure Appl. Chem. **38**, 1231 (2001)
10. D. Katti, K. Robinson, F. Ko, C.J. Laurencin, Biomed. Mater. Res. Part B: Appl. Biomater. **70**, 286 (2004)
11. H. Yoshimoto, Y.M. Shin, H. Terai, J.P. Vacanti, Biomaterials **24**, 2077 (2003)
12. S. Sukigara, M. Gandhi, J. Ayutsede, M. Micklus, F. Ko, Polymer **44**, 5721 (2003)
13. K. Ohgo, C. Zhao, M. Kobayashi, T. Asakura, Polymer **44**, 841 (2003)
14. G. Wnek, M. Carr, D. Simpson, G. Bonlin, Nano. Lett. **3**, 213 (2003)
15. J. Matthews, G. Wnek, D. Simpson, G. Bowlin, Biomacromolecules **3**, 232 (2002)
16. Z.M. Hung, Y.Z. Zhang, S. Ramakrishna, C.T. Lim, Polymer **45**, 5361 (2004)
17. S.K. Chang, D.H. Baek, K.D. Gang, K.H. Lee, I.C. Um, Y.H. Park, Polymer **46**, 5094 (2005)
18. Y.Z. Zhang, H.W. Ouyang, C.T. Lim, S. Ramakrishna, Z.M. Huang, J. Biomed. Mater. Res. Part B: Appl. Biomater. **72**, 156 (2005)
19. S.F. Williams, D.P. Martin, D.M. Horowiz, O.P. Peoples, Int. J. Biol. Macromol. **25**, 111 (1999)
20. K. Maghni, O.M. Nicolescu, J.G. Martin, J. Immunol. Methods **223**, 194 (1999)
21. Y.L. Cui, A.D. Qi, W.G. Liu, X.H. Wang, H. Wang, D.M. Ma, K.D. Yao, Biomaterials **24**, 3859 (2003)
22. L.A. Smith, P.X. Ma, Colloids Surf. B **39**, 125 (2004)
23. C.H. Lee, H.J. Shin, I.H. Cho, Y.M. Kang, I.A. Kimg, K.D. Park, J.W. Shin, Biomaterials **26**, 1261 (2005)
24. H. Tada, O. Shiho, K. Kuroshima, M. Koyama, K. Tsukamoto, J. Immunol. Meth. **93**, 157 (1986)
25. H. Fong, I. Chun, D.H. Reneker, Polymer **49**, 4585 (1999)
26. H. Liu, Y.L. Hseih, J. Polym. Sci. Part B: Polym. Phys. **40**, 2119 (2002)
27. J.M. Deitzel, J.D. Kleinmeyer, J.K. Hirvonen, N.C. Becktan, Polymer **42**, 8163 (2001)
28. Y. Zhang, H. Ouyang, C.T. Lim, S. Ramakrishna, Z.M. Huang, J. Biomed. Mater. Res. B: Appl. Biomater. **72**, 156 (2005)
29. C.M. Chang, C.C. Ko, W.H. Douglass, Biomaterials **24**, 3087 (2003)
30. I.K. Kang, S.H. Choi, D.S. Shin, S.C. Yoon, Int. J. Biol. Macromol. **28**, 205 (2001)
31. J.S. Choi, S.W. Lee, L. Jeong, S.H. Bae, B.C. Min, J.H. Youk, W.H. Park, Int. J. Biol. Macromol. **34**, 249 (2004)
32. M.Y. Li, M.J. Mondrinos, M.R. Gandhi, F.K. Ko, A.S. Weiss, P.I. Lelkes, Biomaterials **26**, 5999 (2005)
33. W. Xia, W. Liu, L. Cui, Y. Liu, W. Zhong, D. Liu, J. Wu, K. Chua, Y. Cao, J. Biomed. Mater. Res. B Appl. Biomater. **71**, 373 (2004)
34. D. Yang, Y. Li, J. Nie, Carbohyd. Polym. **69**, 538 (2007)
35. E.J. Chong, T.T. Phan, I.J. Lim, Y.Z. Zhang, B.H. Bay, S. Ramakrishna, C.T. Lim, Acta. Biomater. **3**, 321 (2007)
36. S.P. Zhong, W.E. Teo, X. Zhu, R. Beuerman, S. Ramakrishna, L.Y.L. Yung, Mat. Sci. Eng. C **27**, 262 (2007)
37. E. Schnell, K. Klinkhammer, S. Balzer, G. Brook, D. Klee, P. Dalton, J. Mey, Biomaterials **28**, 3012 (2007)
38. Z. Chen, X. Mo, F. Qing, Mat. Let. **61**, 3490 (2007)
39. M. Li, Y. Guo, Y. Wei, A.G. Macdiarmid, P.I. Lelkes, Biomaterials **27**, 2705 (2006)
40. J.R. Venugopal, Y. Zhang, S. Ramakrishna, Artif. Organs **30**, 440 (2006)
41. Y. Ito, H. Hasuda, M. Kamitakahera, C. Ohtsuki, M. Tanihara, I.K. Kang, O.H. Kwon, J. Biosci. Bioeng. **100**, 43 (2005)